Transp Porous Med (2012) 92:165–185
DOI 10.1007/s11242-011-9896-5

Efficient Algorithms for Modeling the Transport and Biodegradation of Chlorinated Ethenes in Groundwater

Itza Mendoza-Sanchez · Jeffrey Cunningham

Received: 24 February 2011 / Accepted: 8 October 2011 / Published online: 10 November 2011

Abstract Predicting the fate of chlorinated ethenes in groundwater requires the solution of equations that describe both the transport and the biodegradation of the contaminants. Here, we present a model that accounts for (1) transport of chlorinated ethenes in flowing groundwater, (2) mass transfer of contaminants between mobile groundwater and stationary biofilms, and (3) diffusion and biodegradation within the biofilms. Equations for biodegradation kinetics account for biomass growth within the biofilms, the effect of hydrogen on dechlorination, and competitive inhibition between vinyl chloride and *cis*–dichloroethene. The overall model consists of coupled, non-linear, partial differential equations; solution of such a model is challenging and requires innovative numerical algorithms. We developed and tested two new numerical algorithms to solve the equations in the model; these are called system splitting with operator splitting (SSOS) and system splitting with Picard iteration (SSPI). We discuss the conditions under which one of these algorithms is superior to the other. The contributions of this paper are as follows: first, we believe that the mathematical model presented here is the first transport model that also accounts for diffusion and non-linear biodegradation of chlorinated ethenes in biofilms; second, the SSOS and SSPI are new computational algorithms developed specifically for problems of transport, mass transfer, and non-linear reaction; third, we have identified which of the two new algorithms is computationally more efficient for the case of chlorinated ethenes; and finally, we applied the model to compare the biodegradation behavior under diffusion-limited, metabolism-limited, and hydrogen-limited (donor-limited) conditions.

I. Mendoza-Sanchez
Escuela Superior de Ingeniería y Arquitectura, Instituto Politécnico Nacional, Mexico City, Mexico

Present Address:
I. Mendoza-Sanchez
Department of Civil and Environmental Engineering, Tufts University, Medford, MA, USA
e-mail: Itza.Mendoza-Sanchez@tufts.edu

J. Cunningham (✉)
Department of Civil and Environmental Engineering, University of South Florida, 4202 East Fowler Avenue, Tampa, 33620 FL, USA
e-mail: cunning@usf.edu

Keywords PCE · TCE · DCE · Porous media · Bioremediation · Advection · Dispersion · Reaction kinetics

1 Introduction

Chlorinated ethenes are among the most commonly found contaminants in groundwater. Clean-up of contaminated groundwater, either by natural attenuation or by an engineered approach, often requires predictions of how the target contaminants move and degrade. Such predictions might typically involve solution of an advection-dispersion-reaction equation:

$$\frac{\partial C\,(x,t)}{\partial t} = D\frac{\partial^2 C\,(x,t)}{\partial x^2} - v\frac{\partial C\,(x,t)}{\partial x} + \alpha\,(x,t) \tag{1}$$

where $C(x,t)$ is the concentration of the target contaminant in groundwater, varying as a function of position and time. The three terms on the right-hand side of the equation account for transport of the contaminant by dispersion, transport by advection, and chemical reaction, respectively. For simplicity, we have assumed that transport is primarily one-dimensional in the x direction. Chemical reaction may include degradation (for a parent compound such as perchloroethene), formation (for a final product such as ethene), or both (for intermediate compounds such as trichloroethene, *cis*-dichloroethene (DCE), and vinyl chloride (VC)).

Unfortunately, there are at least two significant problems with Eq. 1. The first problem is that, in many transport models, the kinetics of the biodegradation process are over-simplified. For instance, a typical strategy in a transport model might be to assume first-order kinetics for the formation and degradation of chlorinated ethenes (e.g., Clement et al. 2000; Lu et al. 2003; Sun et al. 2004; An et al. 2004; Beranger et al. 2005). However, a more appropriate description of the reductive dehalogenation of chlorinated ethenes is based on Monod kinetics or Michaelis–Menten kinetics. Studies for reductive dehalogenation have shown the necessity of including substrate limitation, electron-donor limitation, and/or competitive inhibition between chlorinated ethenes on the modeling of bacterial growth (e.g., Ballapragada et al. 1997; Bagley 1998; Fennell and Gossett 1998; Cupples et al. 2004; Yu et al. 2005). Therefore, dechlorination of chlorinated ethenes cannot be well approximated by first-order kinetics. Coupling a non-linear Monod kinetic model to the transport equation (1) is therefore necessary to accurately predict the fate and transport of chlorinated ethenes; some studies in the literature have adopted this approach (e.g., Tompson et al. 1994; El-Farhan et al. 1998).

The second problem with Eq. 1 is that the reaction term α is almost always described in terms of the bulk contaminant concentration, $C(x,t)$. This is a problem because biodegradation typically does not occur in the bulk groundwater, but rather in stationary biofilms that coat the grains of the aquifer solids (Rittmann 1993). In some cases, it may be acceptable to formulate chemical reaction kinetics in terms of the bulk or "macroscopic" concentrations, rather than the concentrations within the biofilm (Baveye and Valocchi 1989). Indeed, Rittmann and VanBriesen (1996) suggested that, in many subsurface applications, "macroscopic" models may be sufficient, and "biofilm" models may be unnecessary. However, Cunningham and Mendoza-Sanchez (2006) demonstrated that using the bulk concentrations to describe biodegradation is acceptable under some circumstances, but not if the biodegradation process is metabolism-limited, that is, if the reaction is slow compared to contaminant mass transfer into the biofilm (Williamson and McCarty 1976). In this case, the biodegradation must be described in terms of the concentrations within the biofilm, not the concentrations in the bulk groundwater (Cunningham and Mendoza-Sanchez 2006). Thus,

although a "macroscopic" formulation may indeed be appropriate in some, perhaps many, circumstances, the more general and complete approach is to account for the fact that biodegradation occurs within biofilms, and hence the mathematical expressions that describe biodegradation must be written in terms of concentrations within those biofilms.

Therefore, in order to accurately predict the transport and biodegradation of chlorinated ethenes, Eq. 1 is likely to be insufficient in many cases. What is required is a model that accounts for at least three important processes: transport in the bulk groundwater, mass transfer between the bulk groundwater and stationary biofilms, and diffusion with non-linear chemical kinetics within the biofilm. This presents a further problem: such a model will involve coupled, non-linear, partial differential equations, and will therefore be difficult to solve efficiently.

In response to these needs, this article makes four important contributions. First, to the best of our knowledge, the mathematical model presented here is the first transport model that also accounts for diffusion and non-linear biodegradation of chlorinated ethenes in biofilms. Second, we present two new computational algorithms developed specifically for problems of transport, mass transfer, and non-linear reaction. Third, we have identified which of the two new algorithms is computationally more efficient for the case of chlorinated ethenes. Finally, we have applied the new model to compare the biodegradation behavior under diffusion-limited, metabolism-limited, and hydrogen-limited (donor-limited) conditions.

2 Mathematical Model

2.1 Transport and Reaction Equations

The purpose of the mathematical model is to describe the transport and degradation of chlorinated ethenes in groundwater. Within the mobile (bulk) groundwater, each chemical species j undergoes advection, dispersion, and mass transfer from the groundwater to a stationary biofilm that coats the grains of the aquifer. These processes are described by Eq. 2.

$$n\,\frac{\partial C_j(x,t)}{\partial t} = n\,D_j\,\frac{\partial^2 C_j(x,t)}{\partial x^2} - n\,v\,\frac{\partial C_j(x,t)}{\partial x} - 3\,(1-n)\,\frac{\omega_j}{R_2} \times \left[C_j(x,t) - S_j\,(x, r = R_2, t)\right] \tag{2}$$

Definitions of all variables are given in Table 1. For simplicity, we assume that sorption and retardation are negligible for the chlorinated ethenes under consideration, though it would be possible to amend Eq. 2 to account for sorption or retardation. Equation (2) has been presented and discussed in the literature previously (e.g., Rosen 1952; Kasten et al. 1952; Rasmuson and Neretnieks 1980; Crittenden et al. 1986) and is therefore not derived here.

We conceptualize that grains of aquifer solids are approximately spherical and are coated by stationary biofilms of uniform thickness (Cunningham and Mendoza-Sanchez 2006; Mendoza-Sanchez and Cunningham 2007). Within the stationary biofilms, each chemical species j undergoes diffusion through the biofilm and chemical reaction.

$$n_f\,\frac{\partial S_j\,(x,r,t)}{\partial t} = n_f D_j^f\,\frac{1}{r^2}\,\frac{\partial}{\partial r}\left[r^2\,\frac{\partial S_j(x,r,t)}{\partial r}\right] + n_f \alpha_j\,(x,r,t) \quad R_1 < r < R_2 \tag{3}$$

Table 1 Definitions of notation in mathematical model, Eqs. 2–9

Symbol	Definition
b	First-order rate coefficient for the death of bacteria in the biofilm (1/T)
$C_j(x,\ t)$	Concentration of chemical species j in the bulk (mobile) groundwater (M/L^3)
D_j	Dispersion coefficient for chemical species j in the bulk groundwater (L^2/T)
D_j^{f}	Diffusion coefficient for chemical species j within the biofilm (L^2/T)
$H(x, r, t)$	Concentration of hydrogen in the biofilm (M/L^3)
H^*	Threshold concentration of hydrogen below which no dechlorination occurs (M/L^3)
K_1	Half-velocity (half-saturation) constant for the biodegradation of DCE (M/L^3)
K_2	Half-velocity (half-saturation) constant for the biodegradation of VC (M/L^3)
K_{H}	Half-velocity (half-saturation) constant for the utilization of hydrogen (M/L^3)
K_{i1}	Coefficient for the inhibition of VC degradation due to competition by DCE (M/L^3)
K_{i2}	Coefficient for the inhibition of DCE degradation due to competition by VC (M/L^3)
n	Bulk porosity of the groundwater aquifer (–)
n_{f}	Porosity of the biofilm (–)
P_{H}	Rate of production of hydrogen by fermentation of electron donors (M/(L^3 T))
q	Maximum utilization rate coefficient for degradation of DCE and VC (1/T)
r	Radial position within the biofilm (L)
R_1	Radius of an aquifer grain, not including the thickness of the biofilm coating the grain (L)
R_2	Radius of an aquifer grain, including the thickness of the biofilm coating the grain (L)
$S_j(x,\ r,\ t)$	Concentration of chemical species j within the biofilm (M/L^3)
t	Time (T)
v	Groundwater velocity (L/T)
x	Position in the bulk groundwater (distance in the direction of mean groundwater flow) (L)
$X(x,\ r,\ t)$	Concentration of biomass in the stationary biofilm (M/L^3)
α_j	Reaction rate of chemical species j (M/(L^3 T))
μ	Maximum bacterial growth rate (1/T)
ω_j	Mass transfer coefficient for chemical j between groundwater and biofilm (L/T)

Equations 2 and 3 are coupled through a boundary condition at the interface between the biofilm and the bulk groundwater, written for each chemical species j.

$$n_{\mathrm{f}} D_j^{\mathrm{f}} \frac{\partial S_j\,(x, r = R_2, t)}{\partial r} = \omega_j \left[C_j\,(x, t) - S_j\,(x, r = R_2, t)\right] \tag{4}$$

Equations analogous to (2–4) have been presented previously (Cunningham and Mendoza-Sanchez 2006; Mendoza-Sanchez and Cunningham 2007; Mendoza-Sanchez 2007), so details of these equations are not repeated here.

It is worth noting that, in this article, we treat the bacteria as a fixed, stationary biofilm. This is a traditional and accepted approach in describing biodegradation in groundwater systems (e.g., Rittmann 1993; Zysset et al. 1994; Lensing et al. 1994; Rittmann and VanBriesen 1996). However, recent experimental data provide conflicting evidence as to the relative importance of mobile (pelagic or planktonic) bacteria in biodegradation of chlorinated ethenes (cf. Schaefer et al. 2009, 2010; Haest et al. 2010). If it becomes clear in the future that mobile bacteria play a significant role in biodegradation of chlorinated ethenes, then the

model presented here will need to be amended to account for both stationary and mobile bacteria, perhaps using a method similar to that employed by Clement et al. (1998).

To the best of our knowledge, the transport equations (2) and (3) have never been coupled to a Monod or Michaelis–Menten model for biodegradation kinetics within the biofilm. In this paper, we adopt the kinetic model developed by Cupples et al. (2004), which describes the reductive dehalogenation of DCE to VC and subsequently to ethene (ETH). This model accounts for biomass growth in the biofilms, competitive inhibition between DCE and VC, and the effect of electron-donor (hydrogen) concentration. The following reaction rate expressions for DCE, VC, and ETH are coupled to Eq. 3.

$$\alpha_{\mathrm{DCE}} = -\left(\frac{q S_{\mathrm{DCE}}(x,r,t)}{S_{\mathrm{DCE}}(x,r,t) + K_1\left(1+\frac{S_{\mathrm{VC}}(x,r,t)}{K_{i2}}\right)}\right)\left(\frac{H(x,r,t)-H^*}{H(x,r,t)-H^*+K_{\mathrm{H}}}\right)X(x,r,t) \tag{5}$$

$$\alpha_{\mathrm{VC}} = -\alpha_{\mathrm{DCE}} - \left(\frac{q S_{\mathrm{VC}}(x,r,t)}{S_{\mathrm{VC}}(x,r,t) + K_2\left(1+\frac{S_{\mathrm{DCE}}(x,r,t)}{K_{i1}}\right)}\right)\left(\frac{H(x,r,t)-H^*}{H(x,r,t)-H^*+K_{\mathrm{H}}}\right)X(x,r,t) \tag{6}$$

$$\alpha_{\mathrm{ETH}} = \left(\frac{q S_{\mathrm{VC}}(x,r,t)}{S_{\mathrm{VC}}(x,r,t) + K_2\left(1+\frac{S_{\mathrm{DCE}}(x,r,t)}{K_{i1}}\right)}\right)\left(\frac{H(x,r,t)-H^*}{H(x,r,t)-H^*+K_{\mathrm{H}}}\right)X(x,r,t) \tag{7}$$

We must also account for how the biomass concentration $X(x,\ r,\ t)$ varies over space and time. In this model, we assume that the thickness of the biofilm is constant in space and time, but that the concentration of active cells within the biofilm can change as bacteria grow or die. Therefore, again following Cupples et al. (2004), we have the following equation for biomass concentration.

$$\frac{\mathrm{d}X(x,r,t)}{\mathrm{d}t} = \mu\left(\frac{S_{\mathrm{DCE}}(x,r,t)}{S_{\mathrm{DCE}}(x,r,t) + K_1\left(1+\frac{S_{\mathrm{VC}}(x,r,t)}{K_{i2}}\right)} + \frac{S_{\mathrm{VC}}(x,r,t)}{S_{\mathrm{VC}}(x,r,t) + K_2\left(1+\frac{S_{\mathrm{DCE}}(x,r,t)}{K_{i1}}\right)}\right) \times \left(\frac{H(x,r,t)-H^*}{H(x,r,t)-H^*+K_{\mathrm{H}}}\right)X(x,r,t) - bX(x,r,t) \tag{8}$$

Unlike the equations for reaction rates of DCE, VC, and ETH (i.e., Eqs. 5–7), the equation for biomass growth (8) is not coupled to a transport equation (3). This is because the biofilms are assumed to be stationary, i.e., fixed films.

Finally, we account for the hydrogen concentration, $H(x,\ r,\ t)$. Hydrogen is produced by the fermentation of electron donors (Fennell and Gossett 1998). By making the simplifying assumption of a spatially and temporally constant hydrogen production rate, P_{H}, we can write the following reaction rate expression for the net production of hydrogen.

$$\alpha_{\mathrm{H}} = P_{\mathrm{H}} - (\alpha_{\mathrm{ETH}} - \alpha_{\mathrm{DCE}})\,. \tag{9}$$

Equation 9 is coupled to Eqs. 2 and 3 to describe the transport, production, and consumption of hydrogen. The assumption of a spatially and temporally constant hydrogen production rate, P_{H}, is a simplification of reality. Accounting for variations in hydrogen production would require the addition of fermentation-related mathematical expressions (e.g., Fennell and Gossett 1998; Hammond et al. 2005), and would also require the model to account for the temporally- and spatially-varying concentration of a fermentable electron donor. Although this may be feasible, it represents a significant increase in the complexity of the model. Experimental data on rates of hydrogen production by fermentation in dechlorinating systems are sparse, and therefore it is not clear that adding this complexity to the model

would improve our predictive capability. In any case, the simplified treatment of hydrogen production employed here was sufficient to qualitatively describe the important behavior of the system under "hydrogen-limited" (donor-limited) conditions, as shown in Sect. 5. Future versions of the model might account for such complexities as variable hydrogen production, variable biofilm thickness, and/or bacterial transport.

Equations 2–9 comprise a model for the transport and reaction of DCE, VC, and ethene. It is worth noting that DCE and VC are daughter products of the biodegradation of trichloroethene (TCE) and/or tetrachloroethene (or perchloroethene, PCE), which are typically the parent compounds at contaminated sites. However, in this paper, we focus only on the conversion of DCE to VC and finally to ethene. As pointed out by Cupples et al. (2004), the conversion of DCE and VC to ethene is often slow, leading to accumulation of these compounds at contaminated sites (e.g., Hoelen et al. 2006). This is especially problematic because VC is the most toxic of the chlorinated ethenes. Hence, a firm understanding of the DCE-to-ethene conversion is warranted. In cases where PCE and TCE are present, the model presented above could be expanded by adding additional equations for the reaction terms α_{TCE} and α_{PCE}, and modifying Eq. 5 to include the formation of DCE by dechlorination of TCE.

2.2 Initial and Boundary Conditions

To complete the model, initial and boundary conditions are required. The initial and boundary conditions may differ depending on the physics of the problem to be considered. Here, we consider the case of contaminated groundwater pumped through columns of porous media, as was described recently elsewhere (Mendoza-Sanchez et al. 2010). The columns are initially considered to contain no contamination. However, we assume that there is a uniform distribution of active bacteria throughout the column, and a uniform concentration of hydrogen (due, for instance, to the fermentation of available electron donors). Therefore, the initial conditions for Eqs. 2, 3, and 8 are as follows.

$$\begin{gathered} C_{\mathrm{DCE}}(x,t=0)=0\ C_{\mathrm{VC}}(x,t=0)=0\ C_{\mathrm{ETH}}(x,t=0)=0\ C_{\mathrm{H}}(x,t=0)=0 \\ S_{\mathrm{DCE}}(x,r,t=0)=0\ S_{\mathrm{VC}}(x,r,t=0)=0\ S_{\mathrm{ETH}}(x,r,t=0)=0\ H(x,r,t=0)=H_0 \\ X(x,r,t=0)=X_0 \end{gathered} \tag{10}$$

We assume that water entering the column is contaminated with *cis*-DCE at a concentration C_0, but does not contain any other contaminant. Thus, the boundary conditions for equation (2) at the upstream end of the column ($x=0$) are as follows.

$$\begin{aligned} &vC_{\mathrm{DCE}}(x=0,t)-D_{\mathrm{DCE}}\frac{\partial C_{\mathrm{DCE}}(x=0,t)}{\partial x}=vC_0 \\ &vC_{\mathrm{VC}}(x=0,t)-D_{\mathrm{VC}}\frac{\partial C_{\mathrm{VC}}(x=0,t)}{\partial x}=0 \\ &vC_{\mathrm{ETH}}(x=0,t)-D_{\mathrm{ETH}}\frac{\partial C_{\mathrm{ETH}}(x=0,t)}{\partial x}=0 \\ &vC_{\mathrm{H}}(x=0,t)-D_{\mathrm{H}}\frac{\partial C_{\mathrm{H}}(x=0,t)}{\partial x}=0 \end{aligned} \tag{11}$$

We also assume that at the effluent end of the column ($x=L$), there is no dispersive flux. Therefore the boundary conditions for Eq. 2 at the downstream end of the column are as follows.

$$D_{\mathrm{DCE}}\frac{\partial C_{\mathrm{DCE}}(x=L,t)}{\partial x}=0 \quad D_{\mathrm{VC}}\frac{\partial C_{\mathrm{VC}}(x=L,t)}{\partial x}=0$$
$$D_{\mathrm{ETH}}\frac{\partial C_{\mathrm{ETH}}(x=L,t)}{\partial x}=0 \quad D_{\mathrm{H}}\frac{\partial C_{\mathrm{H}}(x=L,t)}{\partial x}=0 \tag{12}$$

Finally, we need boundary conditions for Eq. 3. Equation 4 is the boundary condition for Eq. 3 at the surface of the biofilm. The boundary conditions for Eq. 3 at the internal edge of the biofilm (i.e., at $r = R_1$, the interface between the biofilm and the grain which it coats) are as follows.

$$\frac{\partial S_{\mathrm{DCE}}(x,r=R_1,t)}{\partial r}=0 \quad \frac{\partial S_{\mathrm{VC}}(x,r=R_1,t)}{\partial r}=0$$
$$\frac{\partial S_{\mathrm{ETH}}(x,r=R_1,t)}{\partial r}=0 \quad \frac{\partial H(x,r=R_1,t)}{\partial r}=0 \tag{13}$$

Equations 10–13 complete the model that was presented in Eqs. 2–9. With these initial and boundary conditions, it is possible to apply the SSOS or SSPI algorithm to solve the system of equations, and thereby predict the transport of the chemicals through the columns.

2.3 Non-Dimensional Groups

The mathematical model presented in Eqs. 2–13 can be re-written in dimensionless form by non-dimensionalizing the key variables. That results in a reduction of the total number of parameters describing the problem, as parameters in the non-dimensionalized equations appear as dimensionless groups. In the interest of space, we do not here present the full model in dimensionless form. However, a few dimensionless variables or groups are relevant to the ensuing discussion, and hence we define those terms here.

The overall biodegradation process takes place in three steps: mass transfer of the contaminant from the mobile (bulk) groundwater to the biofilm, diffusion through the biofilm, and degradation within the biofilm. The three dimensionless groups that describe those three processes are, respectively, the Stanton number (St_j), the diffusion modulus (Ed_j), and the Damköhler number (Da). There are also separate Damköhler numbers that describe the rates of hydrogen production (Da_{H}), biomass growth (Da_μ), and bacterial death (Da_b). The dimensionless groups Ed_j, Da, and Da_{H} are defined as follows.

$$Ed_j=\frac{D_j^{\mathrm{f}}/R_2^2}{\nu/L} \quad Da=\frac{LqX_0}{\nu C_0} \quad Da_{\mathrm{H}}=\frac{LP_{\mathrm{H}}}{\nu C_0} \tag{14}$$

These three dimensionless groups are particularly important because they characterize if the overall biodegradation process is limited by diffusion in the biofilm, by metabolism of the contaminants, or by production of hydrogen. Note that each chemical (DCE, VC, ETH, hydrogen) can have its own value of the diffusion modulus (Ed_j) because the biofilm diffusion coefficient D_j^{f} may differ for each chemical.

Finally, we note that the time t can be non-dimensionalized according to $\bar{t} = vt/L$. When the model equations are solved numerically (as described below), the time step in the model solution is $\Delta\bar{t} = v\Delta t/L$.

3 Solution Algorithms

Equations 2 and 3 must each be written and solved four times, i.e., for the concentrations of DCE, VC, ETH, and hydrogen. Also, Eq. 8 must be solved for biomass concentration. Thus,

a system of nine coupled, non-linear, partial differential equations must be solved (subject to appropriate boundary and initial conditions). In solving this mathematical model, the goal is to determine the concentrations $C_j(x,t)$ of each chemical species in the bulk groundwater, and the concentrations $S_j(x,r,t)$ of each chemical species within the stationary biofilms. If we know the concentrations C_j and S_j at some time t, then we can estimate the concentrations at $t+\Delta t$ by solving Eqs. 2–9.

Previously, we presented an algorithm (Mendoza-Sanchez and Cunningham 2007) called the system-splitting algorithm, which was capable of efficiently solving equations that describe transport in a bulk phase with diffusion and *linear* reaction kinetics in a stationary phase. That algorithm would be applicable here if the reaction rate terms α_j were linear (e.g., first-order) kinetic expressions. Accounting for *non-linear* reaction kinetics as shown in Eqs. 5–9 requires modification to the system-splitting approach. The essence of the system-splitting approach is that it effectively de-couples the bulk transport equation (2) from the biofilm equation (3), and solves these iteratively until the solutions converge. That framework is still applicable to the current problem, but now a method must be developed to account for the non-linear reaction kinetics in Eq. 3. At least two approaches are possible, as described in the sub-sections that follow.

3.1 System Splitting with Operator Splitting (SSOS)

The first possible approach is to use the system-splitting method while applying operator splitting to solve Eq. 3. Operator splitting has been applied previously to solve problems of transport with reaction (e.g., Chiang et al. 1991; Valocchi and Malmstead 1992; Kaluarachchi and Morshed 1995; Lanser and Verwer 1999). With an operator splitting approach, an approximate solution to Eq. 3 is obtained by de-coupling the diffusion term from the reaction term, and solving these sequentially over small time steps. There is "splitting error" inherently associated with this approach, but the error might be acceptably small if the time steps are small enough (Valocchi and Malmstead 1992).

Figure 1 provides a flow chart of how the SSOS method works to solve for $C_j(x,t+\Delta t)$ and $S_j(x,r,t+\Delta t)$. Here, we describe the procedure briefly in words. For each time step, we make an initial guess at the bulk concentration, the biofilm concentration, and the biomass concentration; these initial guesses are $C^{i=1}(x,t+\Delta t)$, $S^{i=1}(x,r,t+\Delta t)$, and $X^{i=1}(x,r,t+\Delta t)$, respectively. Using the initial guess of $S^{i=1}(x,r=R_2,t+\Delta t)$, we solve Eq. 2 to get an updated estimate of the bulk groundwater concentrations: $C^{i+1}(x,t+\Delta t)$. Then, this updated estimate of bulk groundwater concentration is used in the boundary condition (4), which enables the solution of the *diffusion* part of Eq. 3. The diffusion problem is solved using a standard finite difference approach as described elsewhere (Mendoza-Sanchez and Cunningham 2007; Mendoza-Sanchez 2007). Solution of the diffusion problem provides an intermediate estimate of the biofilm concentration, $S^{\text{diff}}(x,r,t+\Delta t)$. Then, these intermediate concentrations are updated to account for the chemical reactions as given by Eqs. 5–8. The chemical reaction equations are solved using a Runge–Kutta algorithm for ordinary differential equations (Atkinson et al. 1989). This provides updated estimates of the biofilm concentration, $S^{i+1}(x,r,t+\Delta t)$, and the biomass concentration, $X^{i+1}(x,r,t+\Delta t)$. Then, the $(i+1)$th estimates are compared to the ith estimates. If the estimates agree to within a suitable tolerance (as described below), then Eqs. 2 and 3 have been solved successfully for the time step Δt; if the estimates do not agree to within the tolerance, then the entire procedure is repeated, starting with the most recent estimates as an initial guess.

The convergence criterion for the iteration is as follows. For each of the four chemicals considered (DCE, VC, ETH, and hydrogen), we compute the vector of concentration

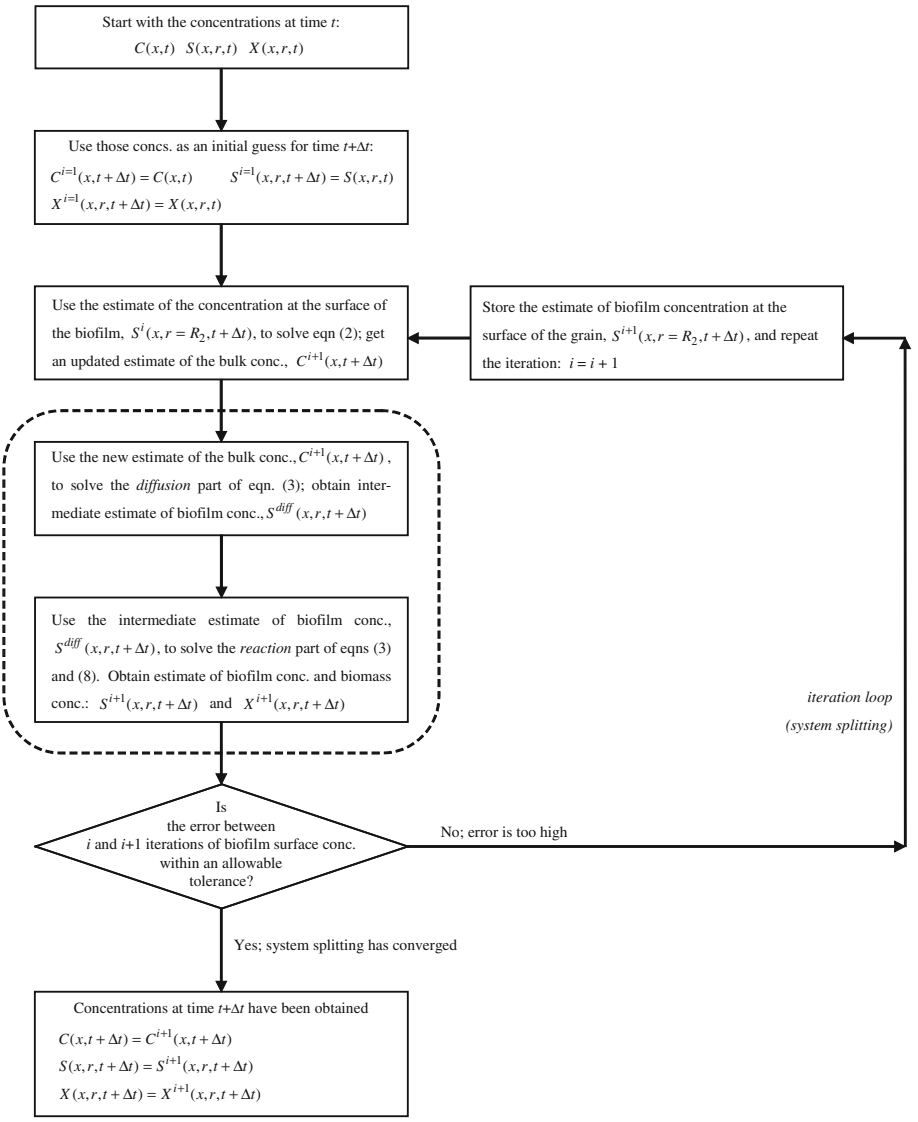

Fig. 1 Flow chart for system splitting with operator splitting (SSOS) approach to solve Eqs. 2–9. Equations 2 and 3 are de-coupled and solved iteratively by the system-splitting approach (Mendoza-Sanchez and Cunningham 2007). In each iteration, Eq. 3 is solved by operator splitting to de-couple the diffusion term from the non-linear reaction term. The *dashed box* indicates the operator-splitting steps

differences $S^{i+1}(x, r = R_2, t + \Delta t) - S^i(x, r = R_2, t + \Delta t)$. Each of those differences is a vector, not a scalar, because there are multiple x locations. We compute the 1-norm of the concentration differences for each of the four chemicals. Then we add together the four 1-norms to provide an overall error. If that overall error is less than 1×10^{-6}, then the iteration has converged.

3.2 System Splitting with Picard Iteration (SSPI)

The second possible approach for solving the mathematical model is to use the system-splitting method while applying Picard iteration (Celia et al. 1990) to solve Eq. 3. Figure 2 provides a flow chart of how the SSPI method works to solve for $C_j(x, t + \Delta t)$ and $S_j(x, r, t + \Delta t)$. The SSPI method is identical to the SSOS method except for the steps indicated by the dashed box in Fig. 2; these steps comprise the Picard iteration algorithm. Here we briefly describe the Picard iteration method with words. The diffusion and reaction terms in Eq. 3 are solved simultaneously, but the reaction terms must be approximated to make this possible. The reaction terms are approximated by using the old (first guess) concentrations inside the biofilm, allowing an approximate solution to Eq. 3, $S^{\text{pred}}(x, r, t + \Delta t)$. Then, the approximate solution of Eq. 3 is used again to obtain a better estimate of the reaction terms. Equation 3 is solved once more using the improved estimate of the reaction terms, yielding a corrected estimate $S^{\text{corr}}(x, r, t + \Delta t)$. This process continues until the solution converges. Thus, the SSPI method involves two iteration loops: an outer iteration loop for the system-splitting approach (which de-couples Eqs. 2 and 3), and an inner iteration loop for the solution of the non-linear diffusion-reaction equation (3).

The convergence criterion for the outer iteration loop (system splitting) was described above in Sect. 3.1. The convergence criterion for the inner iteration loop (the Picard iteration) is as follows. At each x location, we compute vectors of concentration differences, $S^{\text{corr}}(x, r, t + \Delta t) - S^{\text{pred}}(x, r, t + \Delta t)$. That difference is a vector, not a scalar, because there are multiple r locations for each x location. We have four such vectors, one for each chemical (DCE, VC, ETH, and hydrogen). We compute the 1-norm of the concentration differences for each chemical, and we add together the four 1-norms to provide an overall error. If that overall error is less than 1×10^{-6}, then the iteration has converged for that x location. The procedure is repeated for every x location.

3.3 Comparison of SSOS and SSPI methods

The differences between the SSOS and SSPI algorithms can be seen by comparing Fig. 1 to Fig. 2. Steps outside the dashed boxes are identical in the two figures; these represent the steps involved in the system-splitting approach, which is employed in both cases. Steps inside the dashed boxes differ between the two methods; these represent the operator splitting method (in Fig. 1) and the Picard iteration method (in Fig. 2) employed to solve the non-linear diffusion-reaction equations.

Other operator-splitting approaches or iterative approaches may also be possible. These could include Strang splitting, standard sequential iterative splitting, extrapolating sequential iterative splitting, symmetric sequential iterative splitting (Chiang et al. 1991; Valocchi and Malmstead 1992; MacQuarrie and Sudicky 2001; Carrayrou et al. 2004), and/or Newton iteration. Here we limited ourselves to two basic approaches of fundamentally different types (operator splitting vs. iterative non-splitting approach) to assess if one general strategy is superior to the other. Further refinement of the OS or PI methods may be possible in the future but is beyond the scope of this article.

4 Numerical Experiments

Having developed algorithms for solving the mathematical model, two questions arise. First, which of the two methods is more computationally efficient for describing the fate and

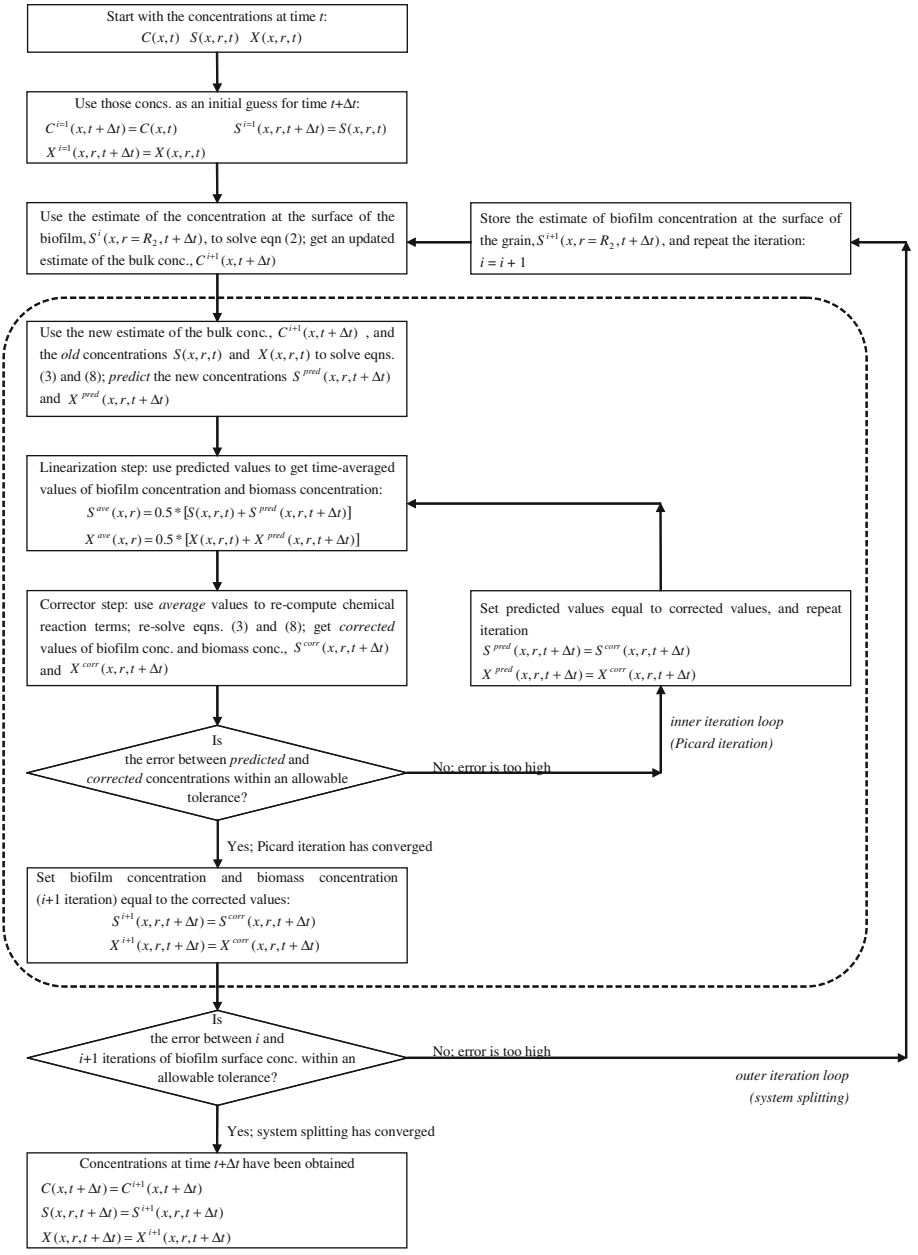

Fig. 2 Flow chart for system splitting with Picard iteration (SSPI) approach to solve Eqs. 2–9. Equations 2 and 3 are de-coupled and solved iteratively by the system-splitting approach (Mendoza-Sanchez and Cunningham 2007). In each iteration, the non-linear diffusion-reaction equation (3) is solved by Picard iteration. The dashed box indicates the steps involved in the Picard iteration method

transport of chlorinated ethenes? Second, what new insights can the model give us regarding the behavior of chlorinated ethenes in the environment? To answer these questions, we have devised a series of numerical experiments, as described in the sub-sections that follow.

Table 2 Test problems for DCE and VC transport and biodegradation

Case	Diffusion rate					Metabolism rate		Hydrogen production rate	
	How fast?	Ed_{DCE}	Ed_{VC}	Ed_{ETH}	Ed_{H}	How fast?	Da	How fast?	Da_{H}
1	Fast	5.22	6.17	7.78	36.5	Fast	7.8	Fast	15
2	Moderate	0.52	0.62	0.78	3.65	Fast	7.8	Fast	15
3	Slow	0.052	0.062	0.078	0.365	Fast	7.8	Fast	15
4	Very slow	0.005	0.006	0.008	0.037	Fast	7.8	Fast	15
5	Fast	5.22	6.17	7.78	36.5	Moderate	1.56	Fast	15
6	Fast	5.22	6.17	7.78	36.5	Slow	0.39	Fast	15
7	Fast	5.22	6.17	7.78	36.5	Very slow	0.078	Fast	15
8	Fast	5.22	6.17	7.78	36.5	Fast	7.8	Moderate	1.5
9	Fast	5.22	6.17	7.78	36.5	Fast	7.8	Slow	0.15
10	Fast	5.22	6.17	7.78	36.5	Fast	7.8	Very slow	0.015

4.1 Comparison of Computational Efficiency

It is not inherently clear which method, SSOS or SSPI, should be more computationally efficient. SSOS requires use of small time steps to keep the splitting error low (Valocchi and Malmstead 1992). SSPI generally allows larger time steps, but requires a number of iterations at each time step. It is possible that one method might be more computationally efficient under certain conditions but not under other conditions. Consider that the overall biodegradation process takes place in three steps: mass transfer of the contaminant from the mobile (bulk) groundwater to the biofilm, diffusion through the biofilm, and metabolism (degradation) within the biofilm. The three dimensionless groups that describe those three processes are, respectively, the Stanton number (St_j), the diffusion modulus (Ed_j), and the Damköhler number (Da). There are also separate Damköhler numbers that describe the rate of hydrogen production (Da_{H}), the rate of biomass growth (Da_{μ}), and the rate of bacterial death (Da_{b}). Thus, the overall rate of biodegradation is influenced by six different rate processes, and depending on the particular values of the dimensionless groups, either the SSOS or the SSPI algorithm might be more computationally efficient.

Therefore, to assess which of these methods is more computationally efficient, we applied both algorithms to 10 test problems. Parameter values selected for the test cases are summarized in Table 2. In all cases, we used the same values of St_j, Da_{μ}, and Da_{b}. However, we varied the values of Ed_j, Da, and Da_{H}; by so doing, we are able to look at cases that are either diffusion-limited, metabolism-limited, or hydrogen-limited. The 10 test cases were formulated to span realistic ranges of the relevant parameters, but are not based on any actual laboratory or field data; rather, the test cases are hypothetical parameter combinations, which are presented to investigate the range of possible model responses.

For each test case, we used both the SSOS and SSPI algorithms to simulate the fate and transport of DCE, VC, and ETH as contaminated water flows through a column of soil. Simulations were performed in the MATLAB® computing environment, version 7.4.0, on a laptop computer with an Intel® Core™2 Duo processor with 2.4 GHz, 4 GB in RAM, and Microsoft Windows®, Vista environment. The "clock" function in MATLAB® was used to quantify the computer time required to run each simulation. To maximize the efficiency of both SSOS and SSPI algorithms, codes were run with the maximum time step Δt that gives an accurate answer; the methods used for determining the maximum allowable Δt are

described in the next section. The efficiency of the algorithms is determined by comparing the computing time that each algorithm required to solve the same test case.

4.2 Determination of Time Step Δt for SSOS and SSPI Algorithms

One of the contributions of this article is the comparison of the SSOS and SSPI algorithms to solve the system of equations presented above. To make a "fair" comparison, both algorithms were implemented with the largest time step, Δt, that would yield a suitably accurate solution; in this fashion, both algorithms were run at maximum efficiency. However, this requires that the maximum allowable Δt be determined for each algorithm for each of the 10 test problems. Here, we describe the procedure by which Δt was determined.

The goal is to select the highest Δt that yields an accurate solution. The difficulty with this is that there is no analytical solution against which we can evaluate the accuracy of the numerical solutions. Thus, for each test case, we proceeded as follows. First, for any test problem under consideration, we ran both the SSOS and SSPI algorithms with a dimensionless time step of $\Delta \bar{t} = 1 \times 10^{-5}$, and as model output, we determined the predicted breakthrough curves of DCE, VC, and ETH. Then, we compared the breakthrough curves predicted by the SSOS algorithm to those predicted by the SSPI algorithm, and we verified that the two algorithms yielded solutions that were essentially identical as determined by a value of the Nash–Sutcliffe model efficiency coefficient (Nash and Sutcliffe 1970) greater than 0.999. These solutions were then accepted as the "correct" solution for the test problem under consideration. Then, for both the SSOS and SSPI algorithms, we re-ran the models with values of Δt higher by a factor of 10, i.e., $\Delta \bar{t} = 1 \times 10^{-4}$, and we compared the new model predictions to the "correct" solutions. If the new model predictions matched the "correct" solution with a Nash–Sutcliffe model efficiency coefficient greater than 0.999, then the time step was again multiplied by a factor of 10, and the process was repeated. If the Nash–Sutcliffe model efficiency coefficient for a simulation generated with a particular value of $\Delta \bar{t}$ was found to be less than 0.999, then that solution was deemed "incorrect," and that value of $\Delta \bar{t}$ was considered to be too large.

To illustrate this procedure, we refer to Figs. 3 and 4. Figure 3 shows predicted breakthrough curves from the SSPI algorithm generated for test problem 1 (see Table 2). The breakthrough curves illustrated are for the sum of the dimensionless DCE, VC, and ETH concentrations at the effluent of the soil columns; hence the breakthrough curves should approach a value of exactly 1 because the total number of DCE, VC, and ETH moles is conserved as DCE is converted to ETH. The breakthrough curves in Fig. 3 were generated with $\Delta \bar{t} = 1 \times 10^{-5}, 1 \times 10^{-4}, \ 1 \times 10^{-3}$, and 1×10^{-2}. In all cases, the breakthrough curves agree, and the value of the Nash–Sutcliffe model efficiency coefficient was effectively 1. Thus, a time step of $\Delta \bar{t} = 1 \times 10^{-2}$ is deemed acceptable for the SSPI algorithm for that test problem, because it matches the "correct" solution. However, Fig. 4 shows breakthrough curves for the same problem, using the same values of $\Delta \bar{t}$, generated with the SSOS algorithm. In this case, when $\Delta \bar{t} = 1 \times 10^{-3}$, the algorithm yields an "incorrect" solution because the splitting error is too large, and the value of the Nash–Sutcliffe model efficiency coefficient is 0.99. Therefore, this solution is rejected. Hence the maximum allowable value of $\Delta \bar{t}$ for the SSOS algorithm is 1×10^{-4} for test problem 1.

4.3 Comparison of Biodegradation under Different Rate-Limiting Conditions

The 10 test cases listed in Table 2 span a range of possible conditions for biodegradation of chlorinated ethenes. Specifically, in cases 2–4, we expect the overall biodegradation process

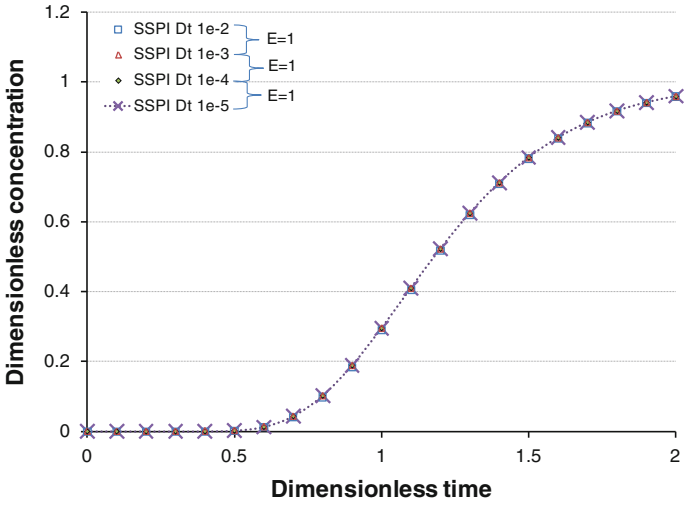

Fig. 3 Breakthrough curves predicted by the SSPI algorithm for test problem 1 using four different values of $\Delta\tilde{t}$. Breakthrough curves are for the sum of the dimensionless DCE, VC, and ETH concentrations at the effluent of the soil columns; hence the breakthrough curves should approach a value of exactly 1 because the total number of DCE, VC, and ETH moles is conserved as DCE is converted to ETH. The parameter E is the Nash–Sutcliffe model efficiency coefficient, which indicates the agreement between two model predictions (Nash and Sutcliffe 1970)

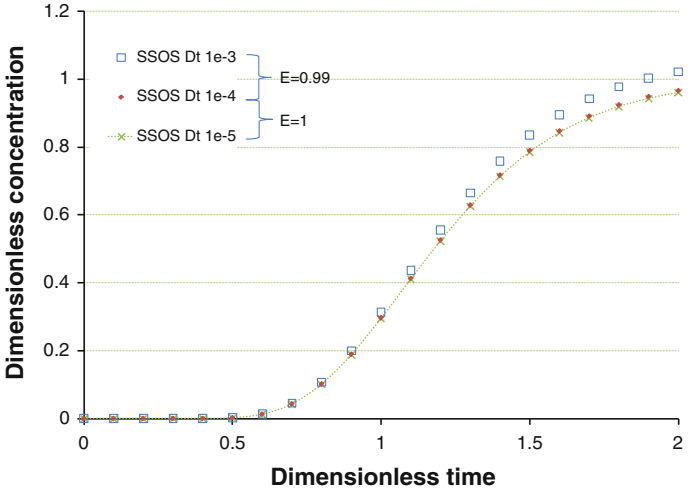

Fig. 4 Breakthrough curves predicted by the SSOS algorithm for test problem 1 using three different values of $\Delta\tilde{t}$. Breakthrough curves are for the sum of the dimensionless DCE, VC, and ETH concentrations at the effluent of the soil columns; hence the breakthrough curves should approach a value of exactly 1 because the total number of DCE, VC, and ETH moles is conserved as DCE is converted to ETH. The parameter E is the Nash–Sutcliffe model efficiency coefficient, which indicates the agreement between two model predictions (Nash and Sutcliffe 1970)

to be limited by the rate of contaminant diffusion through the biofilm; in cases 5–7, we expect biodegradation to be limited by the metabolism of the bacteria within the biofilm; and in cases 8–10, we expect biodegradation to be limited by a low supply of hydrogen (caused,

for instance, by a low supply of fermentable electron donors). The MATLAB® codes that solve Eqs. 2–9 produce, as output, predictions of the breakthrough curves of DCE, VC, and ETH at the exit of the soil columns. Hence, we can compare the predicted breakthrough curves under diffusion-limited, metabolism-limited, and hydrogen-limited (donor-limited) conditions, and we can determine how the overall (macroscopic) biodegradation process depends upon which biofilm-scale process is rate-limiting.

5 Results

5.1 Model and Code Verification

The mathematical model and the computer codes for the SSOS and SSPI algorithms were verified in three ways. First, we verified that the SSOS and SSPI codes predict concentrations that agree to within 10^{-4} % for any given set of input conditions. This indicates that both algorithms are correct (or both contain an error that affects the predicted concentrations identically, which seems very unlikely). Second, we verified that the total number of moles of chemical (i.e., the sum of the DCE moles, the VC moles, and the ethene moles) is conserved during a simulation. Third, we ran test cases where the Monod kinetic parameters were set to a "pseudo-linear" case, i.e., the parameters in Eqs. 5–7 were chosen so that the reaction kinetics are approximately linear (e.g., $C_0 \ll K_1$, $C_0 \gg K_2$, constant H and X); results of simulations with those test cases were verified against our existing linear-kinetics model (Mendoza-Sanchez and Cunningham 2007).

5.2 Comparison of Computational Efficiency

The computing times required by the SSOS and SSPI algorithms for each of the 10 test cases are summarized in Table 3. In some cases, the CPU times are relatively long for a one-dimensional transport simulation. This could be partially a consequence of the hardware (Intel® Core™2 Duo processor with 2.4 GHz, 4 GB in RAM) or the software (MATLAB®) employed. For research purposes, including algorithm development and visualization of results, MATLAB® is chosen because of its user-friendly computing environment. For more complex modeling of 2D or 3D problems, a compiled language with an executable file (such as FORTRAN), and/or a better processor (or cluster of processors), would likely reduce the required computational time. In any case, all simulations reported here were performed on the same computer using the same software, and therefore it is appropriate to compare CPU times between simulations.

As can be seen from Table 3, the two algorithms perform similarly when there is no rate limitation (case 1) or when the biodegradation is metabolism limited (cases 5–7). In these cases, the SSPI can operate at a larger time step, but that advantage is countered by the fact that the SSPI has two iterative loops rather than one, and the net effect is that neither algorithm is markedly superior to the other. However, there are significant differences for cases that are diffusion-limited (cases 2–4) or donor-limited (cases 8–10). Under diffusion-limited conditions, the SSOS requires a small time step to keep the splitting error low, and therefore the SSPI is able to run about 2–10 times faster than the SSOS for cases 2–4. The opposite is true under donor-limited conditions: the SSPI must operate at a small time step in order for the Picard iteration to converge, but the SSOS has no such limitation, and therefore the SSOS is able to run about 40 times faster than the SSPI for cases 8–10. As noted above, codes were run with the maximum time step Δt that gives an accurate answer. This analysis

Table 3 Comparison of computing time for SSOS and SSPI algorithms

case	SSOS algorithm		SSPI algorithm	
	$\Delta\bar{t}$ (dimensionless)	CPU time (h)	$\Delta\bar{t}$ (dimensionless)	CPU time (h)
1	1×10^{-4}	1.24	1×10^{-2}	1.05
2	1×10^{-4}	2.71	1×10^{-2}	1.16
3[a]	1×10^{-4}	5.60	1×10^{-3}	2.76
4[a,b]	1×10^{-5}	55.20	1×10^{-3}	3.91
5	1×10^{-3}	0.43	1×10^{-2}	0.76
6	1×10^{-3}	0.43	1×10^{-2}	0.60
7	1×10^{-3}	0.43	1×10^{-2}	0.57
8	1×10^{-3}	0.47	1×10^{-5}	23.24
9	1×10^{-3}	0.47	1×10^{-5}	20.69
10	1×10^{-3}	0.43	1×10^{-5}	19.67

[a] In cases 1, 2, and 5–10, the biofilm was discretized into 50 radial intervals for solution. However for case 3, the number of radial intervals was 100, and for case 4 the number of radial intervals was 200. Under diffusion-limited conditions, steep concentration fronts may be present in the biofilm, and a finer discretization is required to resolve the steep front.
[b] Case 4 was run to a maximum dimensionless time of $\bar{t} = 1$. All other cases were run to a dimensionless time of $\bar{t} = 2$. A shorter simulation time was implemented for case 4 because the larger number of radial intervals slows down the simulation.

allows users of the model to select which algorithm (SSOS or SSPI) is likely to be superior based on the conditions being simulated.

5.3 Comparison of Biodegradation under Different Rate-Limiting Conditions

Figure 5 shows predicted breakthrough curves (BTCs) for DCE, VC, and ETH for test cases 1, 4, 5, and 8. These BTCs represent predictions of the concentrations of DCE, VC, and ETH that would be observed at the effluent of a soil column fed with DCE-contaminated water. By comparing the BTCs, it is possible to learn something about how the overall biodegradation process is influenced by individual biofilm-scale processes. Case 1 is the "base case" in which all biofilm-scale processes are fast; hence there is no significant limitation to biodegradation, and DCE is converted completely to ethene by the time the water exits the soil column. However, the other three cases each represent a different rate limitation, as summarized in Table 2. Case 4 is characterized by a slow rate of chemical diffusion within the biofilm, i.e., low values of D_j^{f}; case 5 is characterized by a lower value of q, the maximum utilization rate coefficient for degradation of DCE and VC; case 8 is characterized by a lower value of P_{H}, the rate of hydrogen production. Therefore, we refer to cases 4, 5, and 8 as diffusion-limited, metabolism-limited, and hydrogen-limited (or donor-limited), respectively. The terms "diffusion-limited" and "metabolism-limited" have been used in this context previously (Williamson and McCarty 1976).

As seen from Fig. 5, the diffusion-limited and metabolism-limited results are qualitatively similar, but still with some important differences. In both the cases, we see DCE begin to break through, reach a maximum concentration, and then decrease toward a lower value. ETH continues to break through at higher and higher concentrations, and in both cases the system has not reached a steady state even by a dimensionless time $\bar{t} = 4$. This is because

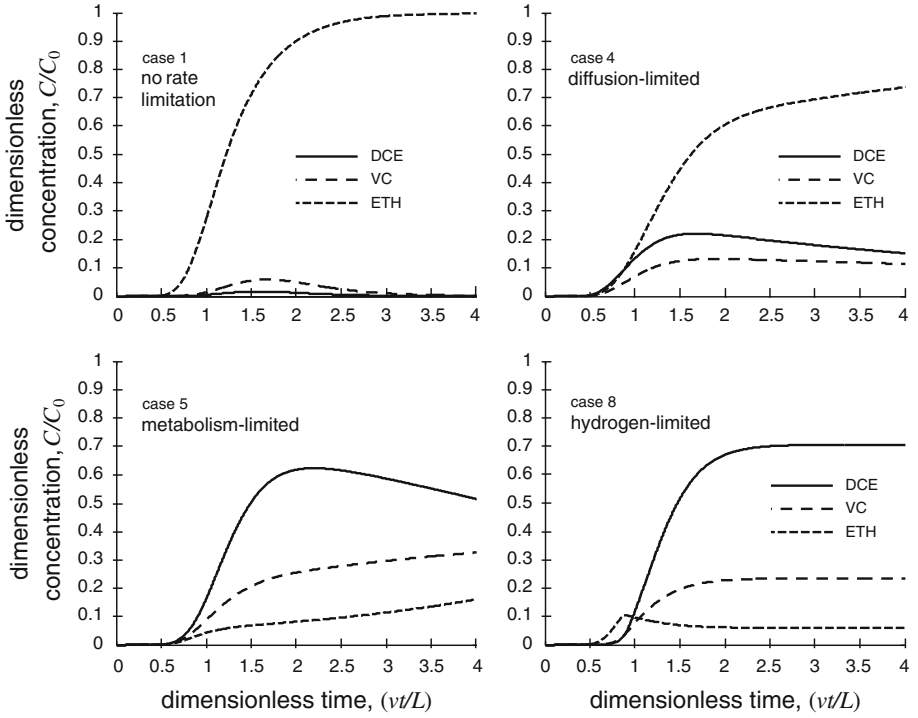

Fig. 5 Breakthrough curves predicted for four of the 10 test cases. Case 1 is the "base case" with no significant limitation to the biodegradation process; case 4 is diffusion-limited (i.e., slow rate of diffusion within the biofilm); case 5 is metabolism-limited; and case 8 is donor-limited (hydrogen-limited)

the microbial population X grows slowly over time, and as X increases, the rates of chemical reaction also increase, as can be seen from Eqs. 5–7. Therefore, diffusion-limited and metabolism-limited conditions are characterized by initial breakthrough of the parent compound, followed by a decrease in the concentration of the parent compound and a continued increase in the concentration of ETH as the overall biodegradation process becomes more efficient. If the simulation had run longer, the system would eventually reach a steady state in which the concentration of DCE breaking through reaches a steady level (results not shown). This behavior has, in fact, been observed in laboratory soil column experiments: see, for instance, Figs. 2f or 3 of Mendoza-Sanchez et al. (2010).

An important difference between case 4 and case 5 is that, in the diffusion-limited case, the biodegradation is still about 80% complete, even though the biofilm diffusion coefficients in case 4 are 1,000 times slower than the corresponding diffusion coefficients in case 1 (as seen in Table 2). Therefore, it appears that biofilm diffusion is not likely to represent a significant limitation to the overall biodegradation process except in very extreme cases, e.g., if the biofilm is very deep. In contrast, decreasing the value of q by a factor of 5 ($Da = 7.8$ in case 1, $Da = 1.6$ in case 5) leads to a significant reduction in the conversion of DCE to ETH. Hence we conclude that the overall biodegradation process is much more sensitive to the specific utilization rate q than to the biofilm diffusion coefficients D_j^{f}.

In the donor-limited case (case 8), the biodegradation of DCE to ETH initially appears successful, with ETH breaking through before DCE. However, after some time, the biodegradation begins to fail, the breakthrough of ETH decreases, and a delayed breakthrough of DCE

is observed. This predicted behavior is somewhat surprising, but it has, in fact, been observed experimentally under conditions that were suspected to be donor-limited: see Figs. 2d or 5 of Mendoza-Sanchez et al. (2010). The critical reason why the biodegradation deteriorates appears to be that the microbial population, X, cannot be sustained without an adequate supply of hydrogen, and as X decreases, the conversion of DCE to ETH deteriorates.

6 Discussion

By formulating and solving the biofilm-scale model presented herein, we gain capabilities that are not available from models based solely on macroscopic concentrations. For instance, the model is able to distinguish subtle differences in contaminant breakthrough behavior depending on what process (biofilm diffusion, contaminant metabolism, or hydrogen production) limits the overall rate. This distinction would not be possible with a model that "lumps" all biofilm-scale processes into a single degradation rate constant.

At least two important implications result from the work presented here. First, with the model presented herein, we might be able to more easily determine what limitation must be overcome in situations where biodegradation of chlorinated ethenes is not observed to be successful. This would improve our ability to clean up contaminated groundwater. Second, application of the model to simulate hydrogen-limited (donor-limited) conditions reveals an important behavior. Biodegradation at first appears successful, with ethene appearing downstream ahead of DCE, but the process later deteriorates and a delayed breakthrough of DCE and VC is observed. This is potentially important because it implies that contaminated groundwater sites must be monitored sufficiently to ensure that successful biodegradation of DCE to ethene is a sustained process and will not fail after some initial apparent success.

There are other biofilm-scale processes not considered in this paper which could also limit the overall rate of biodegradation. These include the mass transfer of the contaminants from the mobile (bulk) groundwater to the surface of the biofilm (i.e., "external" mass transfer) and the growth and death of bacteria within the biofilms. Future work could expand on the analysis presented here to determine the conditions under which those processes have a significant effect on the overall biodegradation process.

The model presented here is intended to extend the modeling capabilities developed previously by other researchers. Space limitations prevent a complete review of all related modeling efforts, but a few of the most salient are considered here. Several previous researchers have developed models that couple the transport of chlorinated ethenes with Monod kinetics or Michaelis–Menten kinetics for biodegradation (e.g., Hossain and Corapcioglu 1996; Clement et al. 1998; El-Farhan et al. 1998; Chambon et al. 2010). However, all of those models estimate reaction rates based on bulk contaminant concentrations, rather than concentrations in biofilms; as noted above, this approach cannot account for differences in behavior between, for instance, diffusion-limited and metabolism-limited conditions. In contrast, other researchers have accounted for diffusion and reaction in biofilms and have coupled those processes to pore-scale (sub-REV-scale) descriptions of flow and transport (e.g., Dillon and Fauci 2000; Eberl et al. 2000). However, such models would need to be "upscaled" in order to produce estimates of macroscopic contaminant behavior, e.g., contaminant breakthrough curves at the column-scale or larger. Bae et al. (1990) developed a model that coupled Darcy-scale transport with diffusion and biodegradation (with Monod kinetics) in biofilms, but it was valid only under steady-state conditions, which allows the use of an effectiveness factor to represent the contaminant flux from bulk fluid into biofilm. Lensing et al. (1994) coupled a transport equation to an equation for biodegradation (Monod kinetics) in a biofilm, but the

biofilm was not spatially resolved, and hence the model of Lensing et al. (1994) would not be able to account for diffusion limitations. Other researchers coupled transport to diffusion and reaction in biofilms, but assumed that the reaction kinetics were linear (e.g., Zysset et al. 1994; Cunningham and Mendoza-Sanchez 2006; Mendoza-Sanchez and Cunningham 2007), which is valid only in specialized circumstances. Thus, overall, to the best of our knowledge, the model presented here is unique in its capabilities.

7 Summary and Conclusions

In this article, we have presented a model that accounts for (1) transport of chlorinated ethenes in flowing groundwater, (2) mass transfer of contaminants between mobile groundwater and stationary biofilms, and (3) diffusion and biodegradation within the biofilms. We have focused on DCE, VC, and ethene, but the model could be easily expanded to also account for tetrachloroethene (perchloroethene) and trichloroethene. Equations for biodegradation kinetics account for biomass growth within the biofilms, the effect of hydrogen on dechlorination, and competitive inhibition between VC and *cis*-dichloroethene. To the best of our knowledge, the mathematical model presented here is the first transport model that also accounts for diffusion and non-linear biodegradation of chlorinated ethenes in biofilms.

To solve the coupled, non-linear, partial differential equations that comprise the mathematical model, we developed and tested two new numerical algorithms to solve the equations in the model. The two new algorithms are extensions of previous work by Mendoza-Sanchez and Cunningham (2007) and are called system splitting with operator splitting (SSOS) and system splitting with Picard iteration (SSPI).

We tested the two solution techniques under different rate-limiting conditions to determine if one algorithm is superior to the other. The two algorithms perform similarly when there is no significant rate limitation or when the biodegradation is metabolism-limited. In these cases, the SSPI can operate at a larger time step, but that advantage is countered by the fact that the SSPI has two iterative loops rather than one, and the net effect is that neither algorithm is markedly superior to the other. Under diffusion-limited conditions, the SSOS requires a small time step to keep the splitting error low, and therefore the SSPI is able to run about 2–10 times faster than the SSOS. The opposite is true under donor-limited conditions: the SSPI must operate at a small time step in order for the Picard iteration to converge, but the SSOS has no such limitation, and therefore the SSOS is able to run about 40 times faster than the SSPI.

Finally, we applied the model to compare the biodegradation behavior under diffusion-limited, metabolism-limited, and hydrogen-limited (donor-limited) conditions. Diffusion-limited and metabolism-limited conditions are both characterized by initial breakthrough of the parent compound, followed by a decrease in the concentration of the parent compound and a continued increase in the concentration of ethene as the overall biodegradation process becomes more efficient. Model results suggest that biofilm diffusion is not likely to represent a significant limitation to the overall biodegradation process except in very extreme cases, e.g., if the biofilm is very deep. The overall biodegradation process was observed to be much more sensitive to the specific utilization rate q than to the biofilm diffusion coefficients D_j^f. In donor-limited conditions, biodegradation initially appears successful, but after some time, the biodegradation begins to fail; this predicted behavior is consistent with previous experimental results (Mendoza-Sanchez et al. 2010). Overall, the model results suggest that processes occurring at the biofilm scale can have important effects on the overall (macroscopic)

biodegradation process, and hence models for biodegradation must incorporate descriptions of these biofilm-scale processes.

Acknowledgments Financial support for this research has been provided to Itza Mendoza-Sanchez from the following sources: Consejo Nacional de Ciencia y Tecnología (CONACYT), México; Instituto Politécnico Nacional (IPN), Ciudad de México, México; and the United States Geological Survey (USGS) through the Texas Water Resources Institute (TWRI). Any opinions, findings, conclusions, or recommendations expressed in this article are those of the authors and do not necessarily reflect the views of CONACYT, IPN, USGS, or TWRI. The authors thank three anonymous reviewers who provided constructive feedback on an earlier version of this article.

References

An, Y.-J., Kampbell, D.H., Weaver, J.W., Wilson, J.T., Jeong, S.-W.: Natural attenuation of trichloroethene and its degradation products at a lake-shore site. Environ. Pollut. **130**, 325–335 (2004)

Atkinson, L.V., Harley, P.J., Hudson, J.D.: Numerical Methods with Fortran 77: A Practical Introduction. Addison-Wesley, Wokingham (1989)

Bae, W., Odencrantz, J.E., Rittmann, B.E., Valocchi, A.J.: Transformation kinetics of trace-level halogenated organic contaminants in a biologically active zone (BAZ) induced by nitrate injection. J. Contam. Hydrol. **6**, 53–68 (1990)

Bagley, D.M.: Systematic approach for modeling tetrachloroethene biodegradation. J. Environ. Eng. (ASCE) **124**, 1076–1086 (1998)

Baveye, P., Valocchi, A.: An evaluation of mathematical models of the transport of biologically reacting solutes in saturated soils and aquifers. Water Resour. Res. **25**, 1413–1421 (1989)

Ballapragada, B.S., Stensel, H.D., Puhakka, J.A., Ferguson, J.F.: Effect of hydrogen on reductive dechlorination of chlorinated ethenes. Environ. Sci. Technol. **31**, 1728–1734 (1997)

Beranger, S.C., Sleep, B.E., Sherwood-Lollar, B., Perez-Monteagudo, F.: Transport, biodegradation and isotopic fractionation of chlorinated ethenes: Modeling and Parameter estimation methods. Adv. Water Resour. **28**, 87–98 (2005)

Carrayrou, J., Moisé, R., Behra, P.: Operator-splitting procedures for reactive transport and comparison of mass balance errors. J. Contam. Hydrol. **68**, 239–268 (2004)

Celia, M.A., Bouloutas, E.T., Zarba, R.L.: A general mass-conservative numerical solution for the unsaturated flow equation. Water Resour. Res. **26**, 1483–1496 (1990)

Chambon, J.C., Broholm, M.M., Binning, P.J., Bjerg, P.L.: Modeling multi-component transport and enhanced anaerobic dechlorination processes in a single fracture-clay matrix system. J. Contam. Hydrol. **112**, 77–90 (2010)

Chiang, C.Y., Dawson, C.N., Wheeler, M.F.: Modeling of in situ biorestoration of organic compounds in groundwater. Transp. Porous Med. **6**, 667–702 (1991)

Clement, T.P., Sun, Y., Hooker, B.S., Petersen, J.N.: Modeling multispecies reactive transport in ground water. Ground Water Monit. Remediat. **18**(2), 79–92 (1998)

Clement, T.P., Johnson, C.D., Sun, Y.W., Klecka, G.M., Bartlett, C.: Natural attenuation of chlorinated ethene compounds: Model development and field-scale application at the Dover site. J. Contam. Hydrol. **42**, 113–140 (2000)

Crittenden, J.C., Hutzler, N.J., Geyer, D.G., Oravitz, J.L., Friedman, G.: Transport of organic compounds with saturated groundwater flow: Model development and parameter sensitivity. Water Resour. Res. **22**(3), 271–284 (1986)

Cunningham, J.A., Mendoza-Sanchez, I.: Equivalence of two models for biodegradation during contaminant transport in groundwater. Water Resour. Res. **42**, W02416 (2006)

Cupples, A.M., Spormann, A.M., McCarty, P.L.: Vinyl chloride and *cis*-dichloroethene dechlorination kinetics and microorganism growth under substrate limiting conditions. Environ. Sci. Technol. **38**, 1102–1107 (2004)

Dillon, R., Fauci, L.: A microscale model of bacterial and biofilm dynamics in porous media. Biotechnol. Bioeng. **68**(5), 536–547 (2000)

Eberl, H.J., Picioreanu, C., Heijnen, J.J., van Loosdrecht, M.C.M.: A three-dimensional numerical study on the correlation of spatial structure, hydrodynamic conditions, and mass transfer and conversion in biofilms. Chem. Eng. Sci. **55**, 6209–6222 (2000)

El-Farhan, Y.H., Scow, K.M., de Jonge, L.W., Rolston, D.E., Moldrup, P.: Coupling transport and biodegradation of toluene and trichloroethylene in unsaturated soils. Water Resour. Res. **34**, 437–445 (1998)

Fennell, D.E., Gossett, J.M.: Modeling the production of and competition for hydrogen in a dechlorinating culture. Environ. Sci. Technol. **32**, 2450–2460 (1998)
Haest, P.J., Springael, D., Smolders, E.: Modelling reactive CAH transport using batch experiment degradation kinetics. Water Res. **44**, 2981–2989 (2010)
Hammond, G.E., Valocchi, A.J., Lichtner, P.C.: Application of Jacobian-free Newton-Krylov with physics-based preconditioning to biogeochemical transport. Adv. Water Resour. **28**, 359–376 (2005)
Hoelen, T.P., Cunningham, J.A., Hopkins, G.D., Lebron, C.A., Reinhard, M.: Bioremediation of *cis*-DCE at a sulfidogenic site by amendment with propionate. Ground Water Monit. Remediat. **26**(3), 82–91 (2006)
Hossain, A., Corapcioglu, M.Y.: Modeling primary substrate controlled biotransformation and transport of halogenated aliphatics in porous media. Transp. Porous Med. **24**(2), 203–220 (1996)
Kaluarachchi, J.J., Morshed, J.: Critical assessment of the operator-splitting technique in solving the advection-dispersion-reaction equation: 1. First-order reaction. Adv. Water Resour. **18**, 89–100 (1995)
Kasten, P.R., Lapidus, L., Amundson, N.R.: Mathematics of adsorption in beds: V. Effect of intraparticle diffusion in flow systems in fixed beds. J. Phys. Chem. **56**(6), 683–688 (1952)
Lanser, D., Verwer, J.G.: Analysis of operator splitting for advection-diffusion-reaction problems from air pollution modeling. J. Comput. Appl. Math. **111**, 201–216 (1999)
Lensing, H.J., Vogt, M., Herrling, B.: Modeling of biologically mediated redox processes in the subsurface. J. Hydrol. **159**, 125–143 (1994)
Lu, X.J., Sun, Y.W., Petersen, J.N.: Analytical solutions of TCE transport with convergent reactions. Transp. Porous Med. **51**, 211–225 (2003)
MacQuarrie, K.T.B., Sudicky, E.A.: Multicomponent simulation of wastewater derived nitrogen and carbon in shallow unconfined aquifers: I. Model formulation and performance. J. Contam. Hydrol. **47**, 53–84 (2001)
Mendoza-Sanchez, I.: Effects of pore-scale velocity and pore-scale physical processes on contaminant biodegradation during transport in groundwater: Modeling and experiments. Ph.D. Dissertation, Texas A&M University, College Station, Texas (2007)
Mendoza-Sanchez, I., Cunningham, J.: Efficient algorithm for modeling transport in porous media with mass exchange between mobile fluid and reactive stationary media. Transp. Porous Med. **68**, 285–300 (2007)
Mendoza-Sanchez, I., Autenrieth, R.L., McDonald, T.J., Cunningham, J.A.: Effect of pore velocity on biodegradation of *cis*-dichloroethene (DCE) in column experiments. Biodegradation **21**, 365–377 (2010)
Nash, J.E., Sutcliffe, J.V.: River flow forecasting through conceptual models part I—a discussion of principles. J. Hydrol. **10**(3), 282–290 (1970)
Rasmuson, A., Neretnieks, I.: Exact solution of a model for diffusion in particles and longitudinal dispersion in packed beds. AIChE J. **26**(4), 686–690 (1980)
Rittmann, B.E.: The significance of biofilms in porous media. Water Resour. Res. **29**, 2195–2202 (1993)
Rittmann, B.E., VanBriesen, J.M.: Microbiological processes in reactive modeling. In: Lichtner, P.C., Steefel, C.I., Oelkers, E.H. (eds.) Reactive Transport in Porous Media, vol. 34. Reviews in Mineralogy, pp. 311–334. Mineralogical Society of America, Chantilly, VA (1996)
Rosen, J.B.: Kinetics of a fixed bed system for solid diffusion into spherical particles. J. Chem. Phys. **20**(3), 387–394 (1952)
Schaefer, C.E., Callaghan, A.V., King, J.D., McCray, J.E.: Dense nonaqueous phase liquid architecture and dissolution in discretely fractured sandstone blocks. Environ. Sci. Technol. **43**(6), 1877–1883 (2009)
Schaefer, C.E., Towne, R.M., Vainberg, S., McCray, J.E., Steffan, R.J.: Bioaugmentation for treatment of dense non-aqueous phase liquid in fractured sandstone blocks. Environ. Sci. Technol. **44**(13), 4958–4964 (2010)
Sun, Y., Lu, X., Petersen, J.N., Buscheck, T.A.: An analytical solution of tetrachloroethylene transport and biodegradation. Transp. Porous Med. **55**, 301–308 (2004)
Tompson, A.F.B., Knapp, R.B., Hanna, M.L., Taylor, R.T.: Simulation of TCE migration and biodegradation in a porous medium under conditions of finite degradation capacity. Adv. Water Resour. **17**, 241–249 (1994)
Valocchi, A.J., Malmstead, M.: Accuracy of operator splitting for advection-dispersion-reaction problems. Water Resour. Res. **28**, 1471–1476 (1992)
Williamson, K., McCarty, P.L.: A model of substrate utilization by bacterial films. J. Water Pollut. Control Fed. **48**, 9–24 (1976)
Yu, S.H., Dolan, M.E., Semprini, L.: Kinetics and inhibition of reductive dechlorination of chlorinated ethylenes by two different mixed cultures. Environ. Sci. Technol. **39**, 195–205 (2005)
Zysset, A., Stauffer, F., Dracos, T.: Modeling of reactive groundwater transport governed by biodegradation. Water Resour. Res. **30**(8), 2423–2434 (1994)